Supplementary Material for Hahn et al. (2021)

Table S1. Models Included in Analysis

CMIP5 Models (28)	CMIP6 Models (42)	AMIP6 Models (38)
ACCESS1-0	ACCESS-CM2	ACCESS-CM2
ACCESS1-3	ACCESS-ESM1-5	ACCESS-ESM1-5
BNU-ESM	AWI-CM-1-1-MR	BCC-CSM2-MR
CCSM4	BCC-CSM2-MR	CESM2
CNRM-CM5	BCC-ESM1	CESM2-FV2
CSIRO-Mk3-6-0	CAMS-CSM1-0	CESM2-WACCM
CanESM2	CESM2	CESM2-WACCM-FV2
FGOALS-g2	CESM2-FV2	CMCC-CM2-HR4
FGOALS-s2	CESM2-WACCM	CMCC-CM2-SR5
GFDL-CM3	CESM2-WACCM-FV2	CNRM-CM6-1
GFDL-ESM2G	CMCC-CM2-SR5	CNRM-CM6-1-HR
GFDL-ESM2M	CMCC-ESM2	CNRM-ESM2-1
GISS-E2-H	CNRM-CM6-1	CanESM5
GISS-E2-R	CNRM-CM6-1-HR	E3SM-1-0
HadGEM2-ES	CNRM-ESM2-1	EC-Earth3
IPSL-CM5A-MR	CanESM5	EC-Earth3-AerChem
IPSL-CM5B-LR	E3SM-1-0	EC-Earth3-CC
MIROC-ESM	EC-Earth3	EC-Earth3-Veg
MIROC5	EC-Earth3-AerChem	FGOALS-f3-L
MPI-ESM-LR	EC-Earth3-Veg	FGOALS-g3
MPI-ESM-MR	FGOALS-f3-L	GFDL-CM4
MPI-ESM-P	FGOALS-g3	GISS-E2-1-G
MRI-CGCM3	GFDL-CM4	IITM-ESM
NorESM1-M	GFDL-ESM4	INM-CM4-8
NorESM1-ME	GISS-E2-1-G	INM-CM5-0
bcc-csm1-1	GISS-E2-1-H	IPSL-CM6A-LR
bcc-csm1-1-m	HadGEM3-GC31-LL	KACE-1-0-G
inmcm4	HadGEM3-GC31-MM	MIROC6
	INM-CM4-8	MPI-ESM-1-2-HAM
	INM-CM5-0	MPI-ESM1-2-HR
	IPSL-CM6A-LR	MPI-ESM1-2-LR
	MIROC-ES2L	MRI-ESM2-0
	MIROC6	NESM3
	MPI-ESM-1-2-HAM	NorCPM1
	MPI-ESM1-2-HR	NorESM2-LM
	MPI-ESM1-2-LR	SAM0-UNICON
	MRI-ESM2-0	TaiESM1
	NorCPM1	UKESM1-0-LL
	NorESM2-MM	
	SAM0-UNICON	
	TaiESM1	
	UKESM1-0-LL	

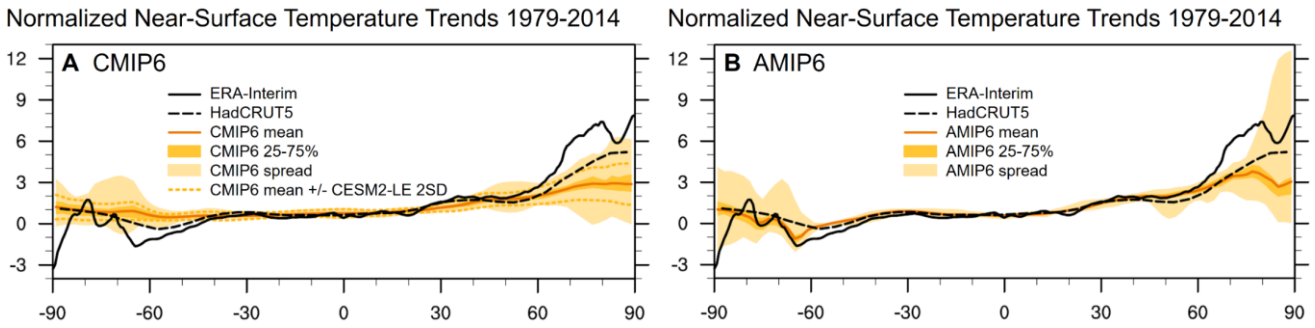

Figure S1. Annual-mean near-surface temperature trends normalized by the global-mean trend for 1979-2014 in the ERA-Interim reanalysis (solid black line), HadCRUT5 observations (dashed black line), and the historical CMIP6 (A) and AMIP6 (B) multimodel means (solid orange line). The dark orange shading shows the 25th to 75th percentiles, and the light orange shading shows the full intermodel spread. The dashed orange lines (A) show the CMIP6 mean +/- 2 standard deviations across ensemble members in the CESM2-LE.

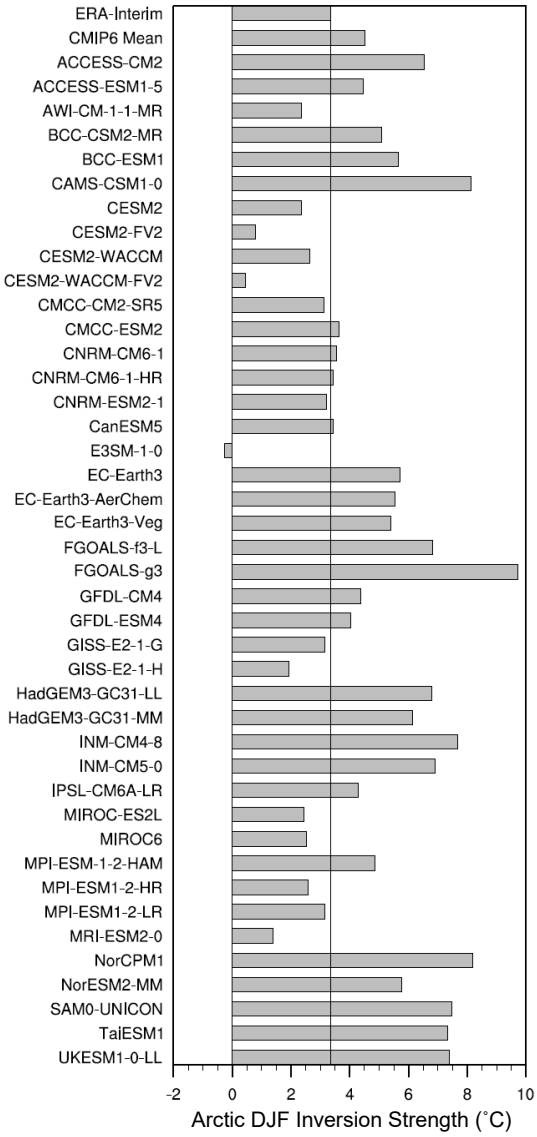

Figure S2. December-January-February (DJF) Arctic mean inversion strength (˚C) for 1979-2014 in the ERA-Interim reanalysis and CMIP6 models. Inversion strength is defined as the 850 hPa temperature minus the near-surface air temperature for each gridpoint and month before time- and area-averaging. Black vertical line shows the Arctic DJF inversion strength for ERA-Interim.

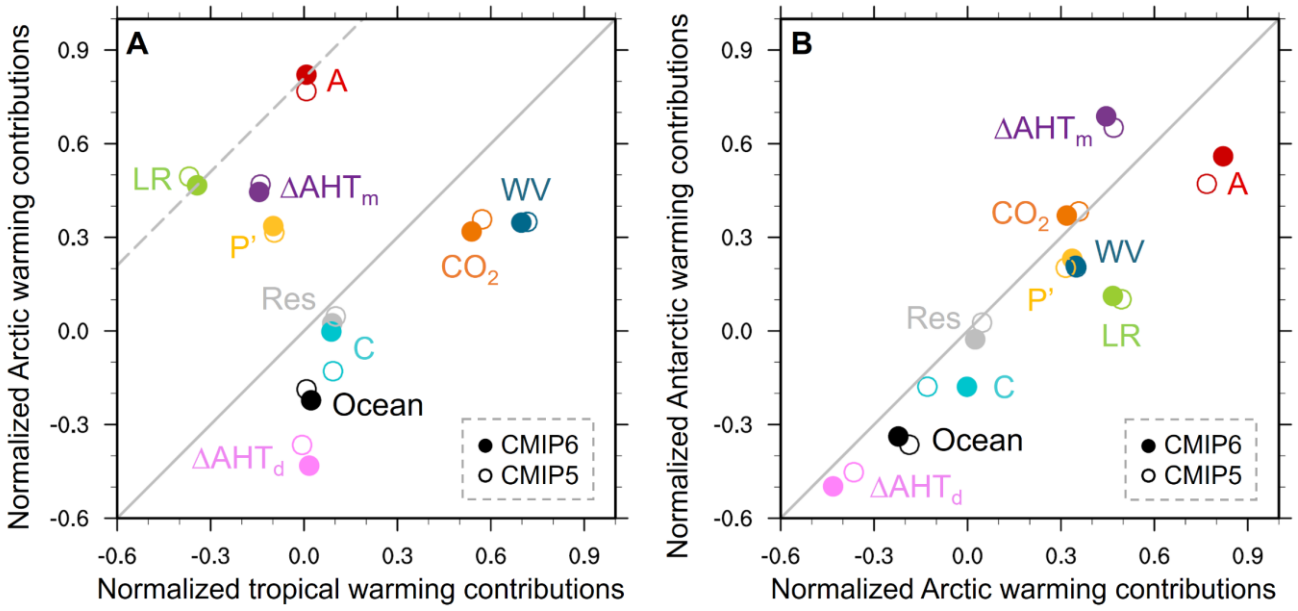

Figure S3. Contributions of each feedback and atmospheric forcing to warming centered around year-100 of abrupt CO_2 quadrupling in CMIP6 (filled circles) and CMIP5 (hollow circles) for (A) the tropics relative to the Arctic and (B) the Arctic relative to the Antarctic, with regional warming contributions normalized by the global-mean near-surface warming. Warming contributions are shown for the lapse-rate (LR), surface albedo (A), water-vapor (WV), and cloud (C) feedbacks, the variation in the Planck response from its global-mean value (P'), effective radiative forcing (CO_2), change in moist and dry AHT convergence (ΔAHT_m; ΔAHT_d) and ocean heat uptake (Ocean), and residual term (Res). Dashed grey line shows a 1-to-1 slope through the normalized lapse-rate feedback warming contribution.

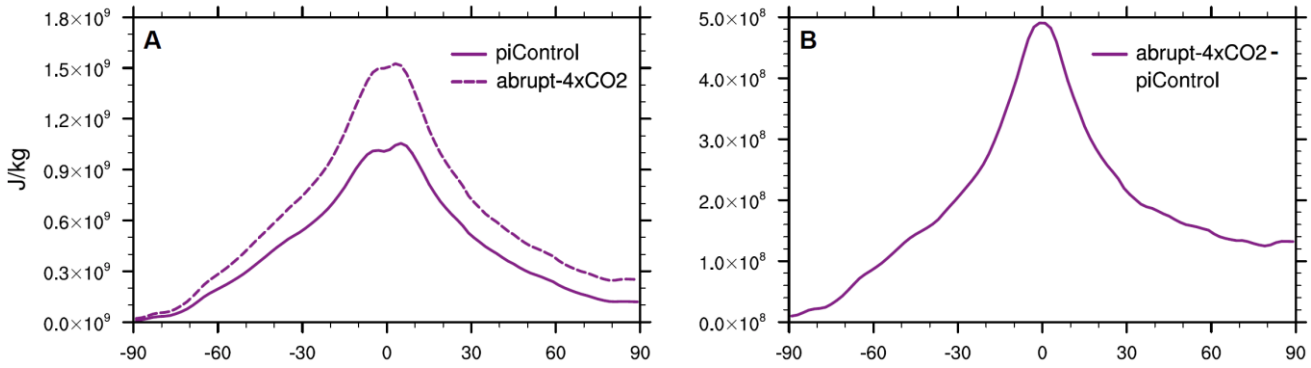

Figure S4. Annual-mean latent energy component of the moist static energy (J/kg) in the CMIP6 multimodel mean, equal to the vertically-integrated specific humidity (weighted by pressure level thickness) multiplied by the latent heat of vaporization. Latent energy is averaged over 31 years centered on year-100 in the abrupt CO_2 quadrupling (A; dashed line) and preindustrial control (A; solid line) experiments and their difference (B).

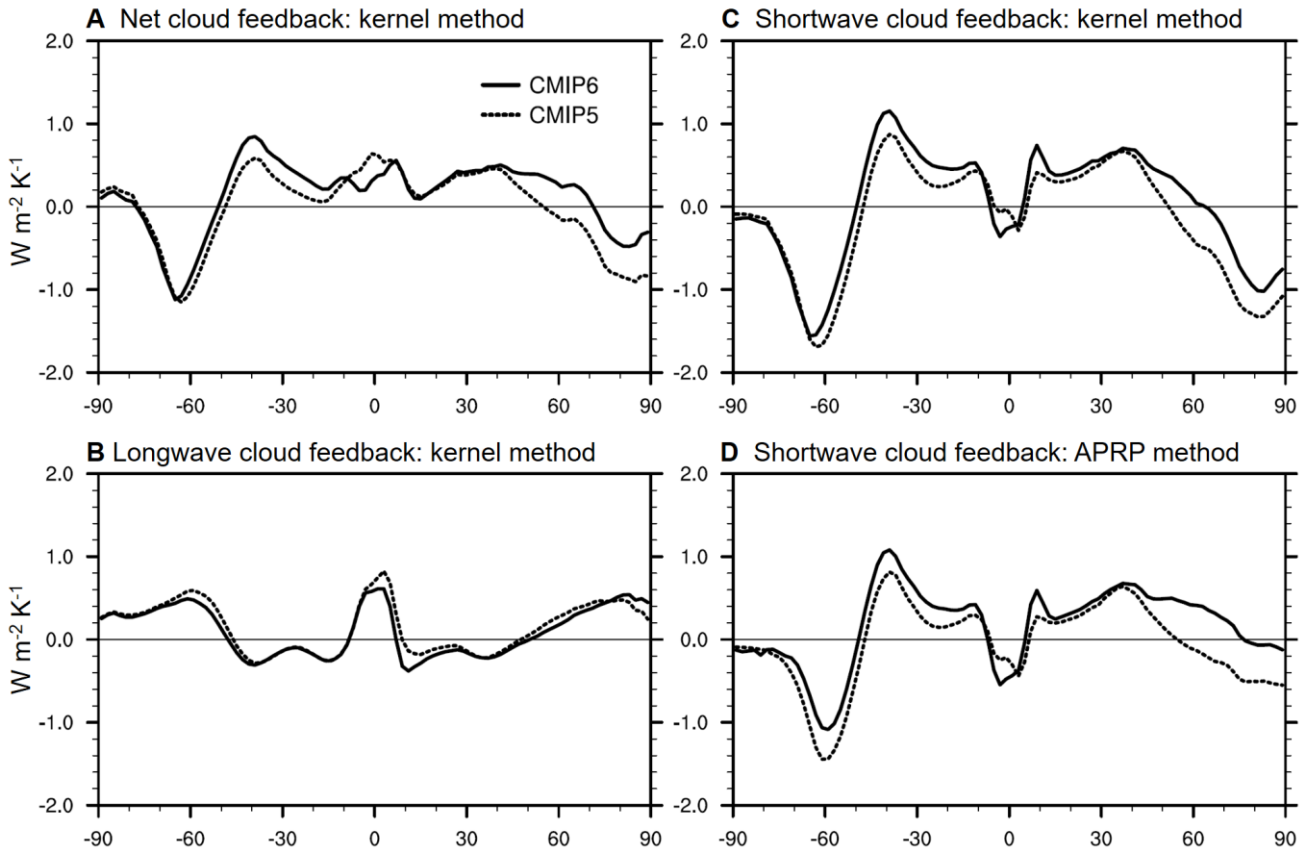

Figure S5. Annual- and zonal-mean cloud feedbacks (W m^{-2} K^{-1}) calculated using the year-100 radiative anomalies contributed by cloud feedbacks at each gridpoint divided by the year-100 annual- and global-mean near-surface temperature anomalies under CO_2 quadrupling. Dashed (solid) line shows the CMIP5 (CMIP6) multimodel mean for (A) the kernel-derived net cloud feedback, (B) the kernel-derived longwave cloud feedback, (C) the kernel-derived shortwave cloud feedback, and (D) the shortwave cloud feedback calculated with the APRP method of Taylor et al. (2007).

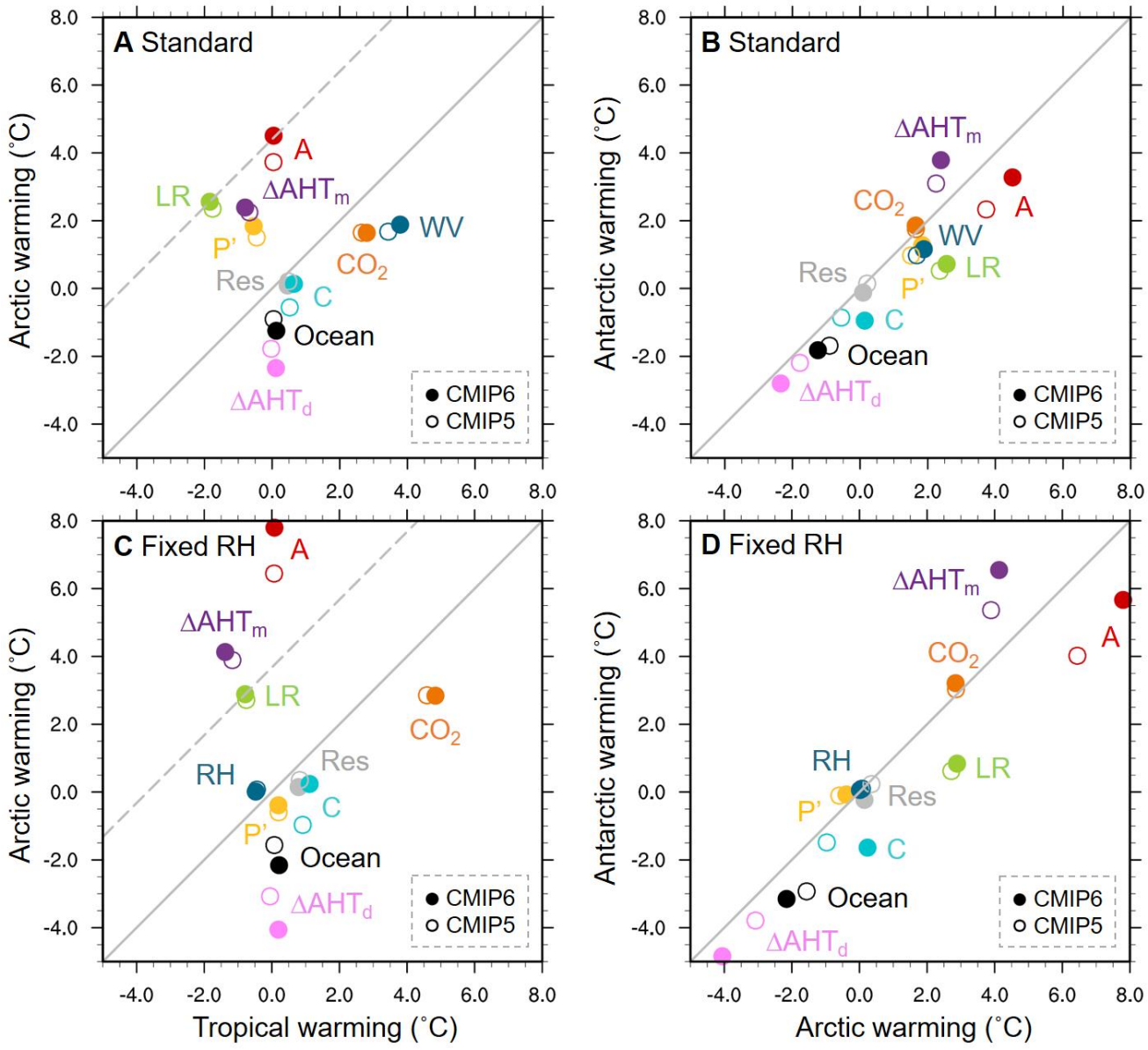

Figure S6. Contributions to warming (˚C) centered around year-100 of abrupt CO_2 quadrupling in CMIP6 (filled circles) and CMIP5 (hollow circles) for (A, C) the tropics relative to the Arctic and (B, D) the Arctic relative to the Antarctic, using (A, B) the standard kernel method, as in Figure 4, compared to (C, D) the fixed RH method. Warming contributions are shown for the lapse-rate (LR), surface albedo (A), water-vapor (WV), and cloud (C) feedbacks, the variation in the Planck response from its global-mean value (P'), effective radiative forcing (CO_2), change in moist and dry AHT convergence (ΔAHT_m; ΔAHT_d) and ocean heat uptake (Ocean), and residual term (Res). Dashed grey line shows a 1-to-1 slope through the lapse-rate feedback warming contribution.

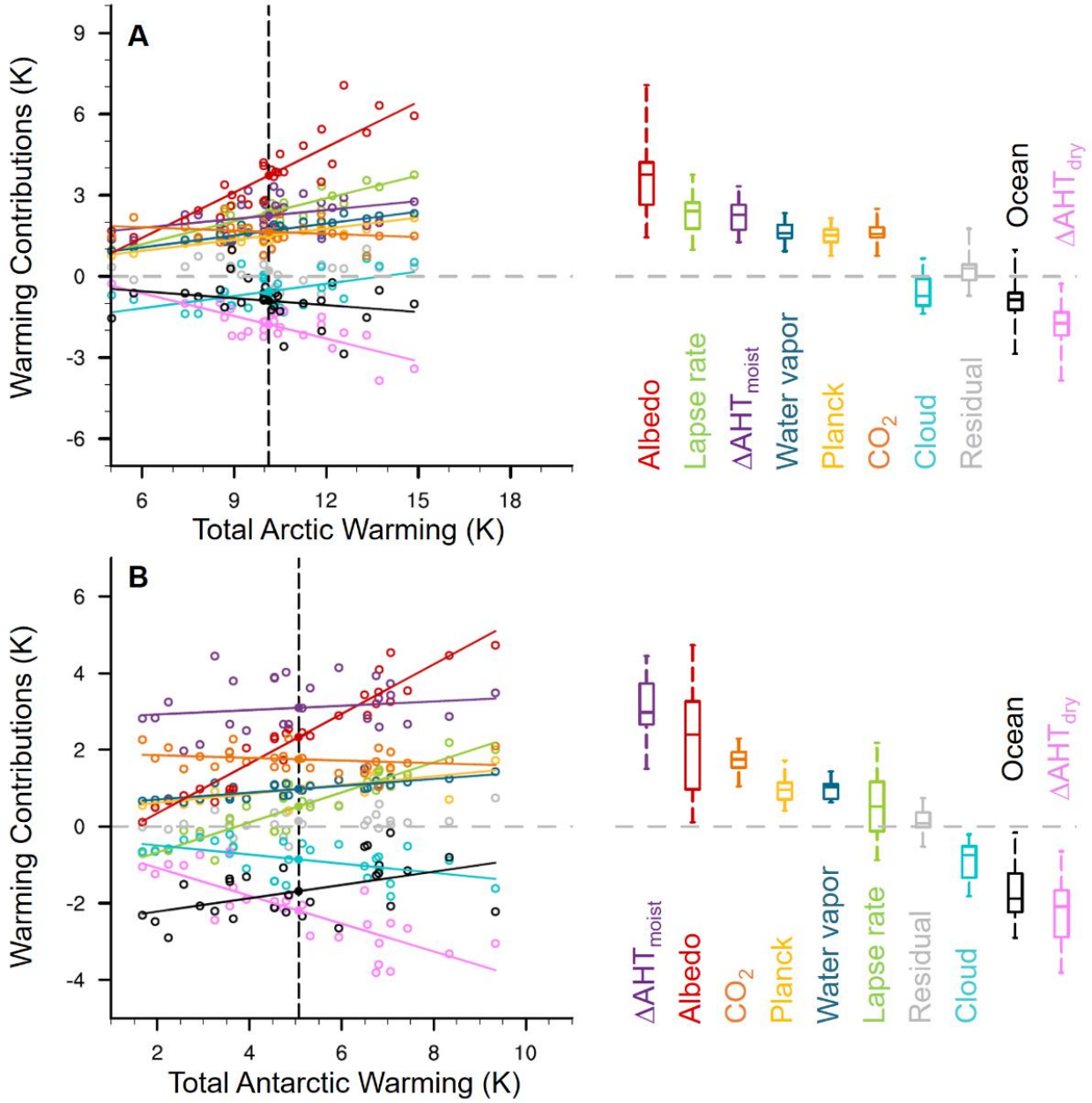

Figure S7. Intermodel spread of warming contributions versus total warming (˚C) in individual models for (A) the Arctic and (B) the Antarctic in CMIP5. Solid lines show linear regressions of feedback contributions against total warming at each pole. Filled circles on the black dashed line show the CMIP5 intermodel mean. In the right-hand panel, boxes indicate the median and 25th and 75th percentiles, and whiskers show the full intermodel spread of polar warming contributions.

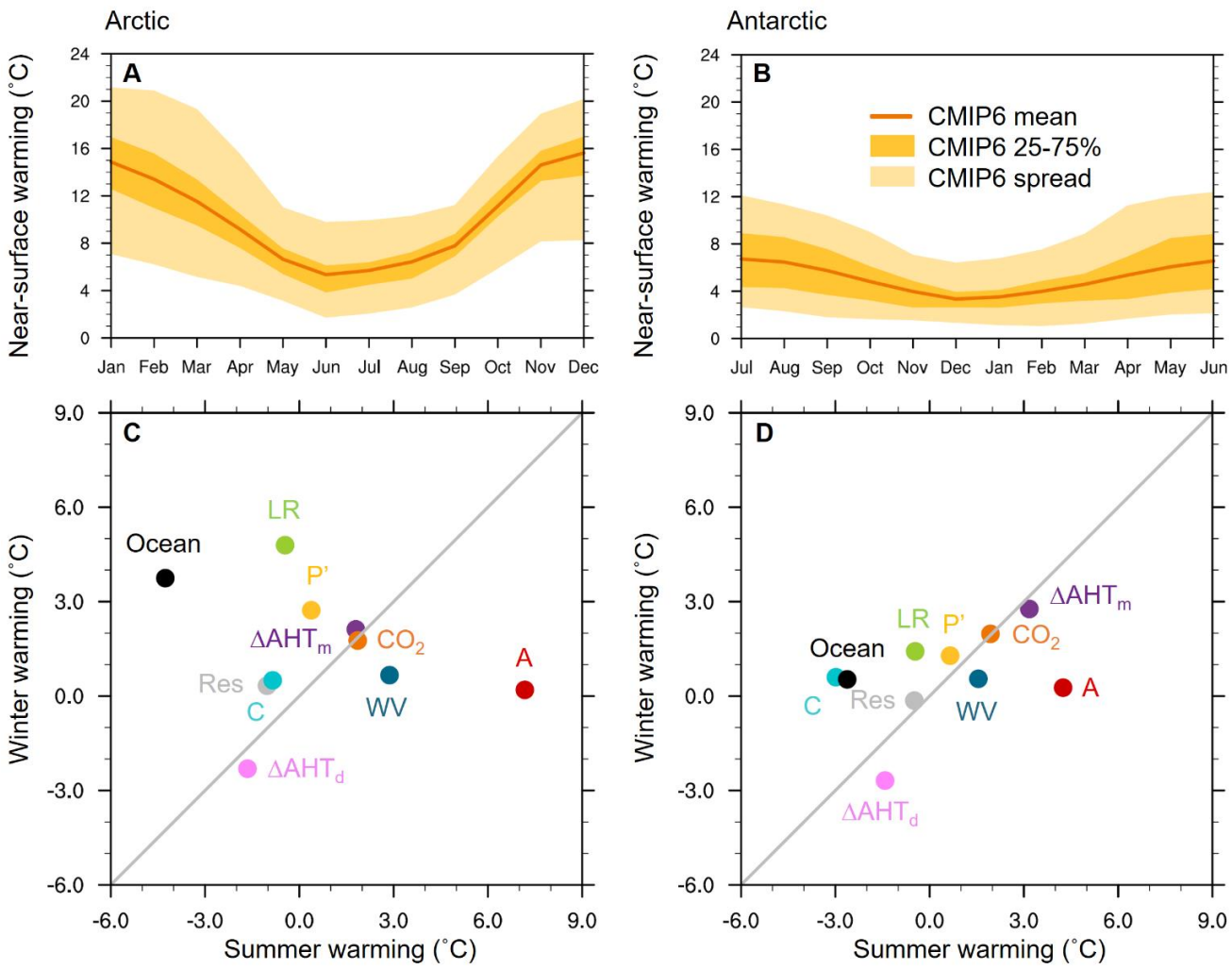

Figure S8. Monthly near-surface warming (˚C) centered around year-100 of abrupt CO_2 quadrupling for the CMIP5 multimodel mean (orange line), the 25th to 75th percentile (dark orange shading), and the full intermodel spread (light orange shading) in (A) the Arctic and (B) the Antarctic. (C, D) Contributions of each feedback and atmospheric forcing to winter and summer warming (˚C) centered around year-100 of abrupt CO_2 quadrupling in CMIP5 for (C) the Arctic and (D) the Antarctic. Warming contributions are shown for the lapse-rate (LR), surface albedo (A), water-vapor (WV), and cloud (C) feedbacks, the variation in the Planck response from its global-mean value (P'), effective radiative forcing (CO_2), change in moist and dry AHT convergence (ΔAHT_m; ΔAHT_d) and ocean heat transport and storage (Ocean), and residual term (Res).

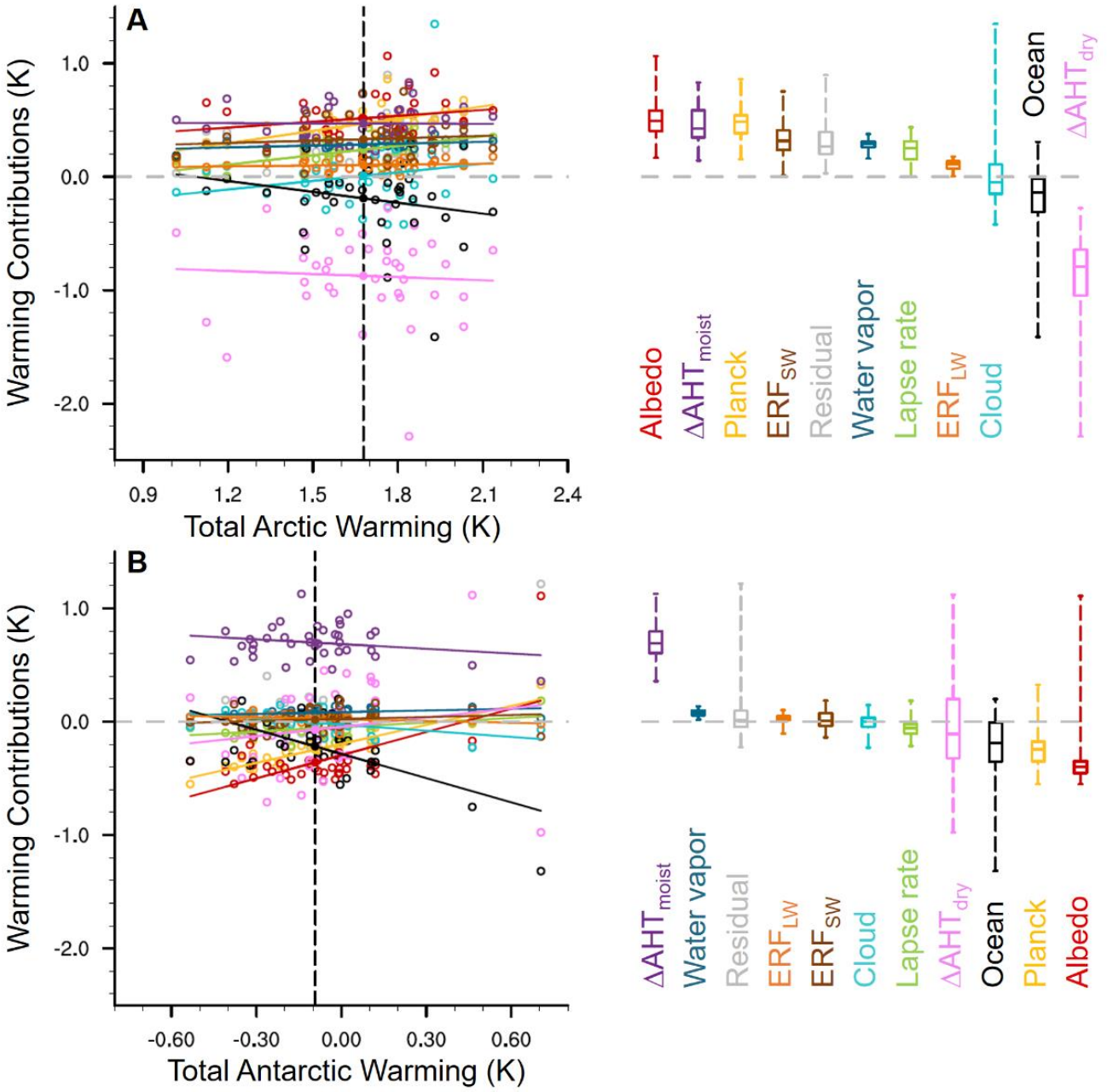

Figure S9. Intermodel spread of warming contributions versus total warming (˚C) in individual models for (A) the Arctic and (B) the Antarctic for 1979-2014 in AMIP6. Solid lines show linear regressions of feedback contributions against total warming at each pole. Filled circles on the black dashed line show the AMIP6 intermodel mean. In the right-hand panel, boxes indicate the median and 25th and 75th percentiles, and whiskers show the full intermodel spread of polar warming contributions.